# PULSE NUCLEAR MAGNETIC RESONANCE MEASUREMENTS OF WATER EXCHANGE ACROSS THE ERYTHROCYTE MEMBRANE EMPLOYING A LOW Mn CONCENTRATION

JAMES L. PIRKLE, DAVID L. ASHLEY, AND J. H. GOLDSTEIN, *Department of Chemistry and School of Medicine, Emory University, Atlanta, Georgia 30322 U.S.A.*

ABSTRACT A simple, precise, and rapid pulse nuclear magnetic resonance technique for measuring the rate of water exchange across the erythrocyte membrane is presented. The technique is based upon the nonlinear fit of Carr-Purcell-Meiboom-Gill (CPMG) transverse relaxation time data of blood doped with 1.7 mM $MnCl_2$ to the general two-compartment exchange equation. Previous approaches using CPMG data required high $MnCl_2$ concentrations (25–53 mM), shown in this work to induce systematic errors ranging from 35 to 45%. At 23°C the average residence time of a water molecule inside the erythrocyte ($\tau_a$) is 21.0 ± 0.6 ms (SE). The Arrhenius plot for water exchange is linear over the range of 3°–37°C and the Arrhenius activation energy is 4.79 ± 0.03 kcal (SE). This value does not differ significantly from the energy required for bulk water flow. Results are compared with previous determinations, and sources of systematic error in $\tau_a$ and the activation energy are evaluated.

## INTRODUCTION

The mechanism of water transport across a biological membrane is not clearly understood (1–5, 10). Such fundamental knowledge would obviously apply in understanding many physiological processes, ranging from regulation of cell volume to the protection of cells undergoing cryogenic preservation. The relative simplicity and availability of erythrocytes have made them a primary target for investigation of how water enters and leaves the cell. Measurements of the rate of water exchange across the erythrocyte membrane have been used to establish and evaluate models of the water transport mechanism. It is therefore important to consider the accuracy of such measurements carefully.

The two main techniques used to measure water exchange across the erythrocyte membrane are isotope tracer and nuclear magnetic resonance (NMR). The isotope tracer method involves a fairly elaborate flow tube apparatus and a rather exacting experimental procedure of mixing and sampling and about 50 ml of blood (6). These factors tend to prohibit the routine application of this method. In addition, the tracer method is complicated by errors introduced from unstirred layers adjacent to the membrane (7).

The NMR technique has focused on measuring nuclear spin magnetization in an analogous fashion to the standard $T_1$ and $T_2$ relaxation measurements (8). For the sake of simplicity, the exchange measurement analogous to the $T_1$ experiment will be called a "$T_1$-type experiment" and similarly with $T_2$. These measurements are made at equilib-

BIOPHYS. J. © Biophysical Society · 0006-3495/79/03/389/18 $1.00
Volume 25 March 1979 389–406

rium (avoiding the unstirred layer problem) and require <0.5 ml of blood. The determination of the water exchange rate in a $T_1$- or $T_2$-type experiment involves the use of fairly complex equations, which relate the measured net magnetization to the exchange rate of water molecules between the intracellular and plasma compartments.

The $T_1$-type experiments have used both the nuclei of hydrogen (the proton) and the $^{17}O$ isotope, whereas the $T_2$-type experiment has been applied only to protons. The $T_1$-type $^{17}O$ measurement turns out to have limited usefulness because it is sensitive to the exchange rate over only a narrow temperature range (9). For the $T_1$- or $T_2$-type measurements of water protons to be sufficiently sensitive to the exchange rate of water across the erythrocyte membrane, it is necessary to dope the plasma with a paramagnetic substance, e.g., $MnCl_2$, which shortens the relaxation time of water in the plasma compartment. Most workers have employed high concentrations (20–53 mM) of $MnCl_2$ in the plasma, which reduces the complex general exchange expression considerably and thus simplifies data analysis. Unfortunately, results from this study indicate that these high $MnCl_2$ concentrations induced a systematic error of between 35 and 45% in the measurement of the exchange rate. It is therefore important to note that if the more general form of the exchange equations is used, a low $MnCl_2$ concentration ($\cong$1.7 mM) is sufficient to enable the exchange rate to be calculated. To date, only a $T_1$-type experiment has been reported using this low $MnCl_2$ concentration approach. This work presents the results of employing the $T_2$-type technique with the plasma doped with low concentrations of $MnCl_2$ and the data analyzed by the complete two-compartment exchange equation.

This $T_2$-type technique retains all the advantages of the $T_1$-type and offers several additional advantages. First, the $T_2$ technique is much faster. With our experimental set up, every 3 s, 500 points can be measured to define a line shape from which the exchange rate can be calculated. To obtain a line shape of comparable quality from $T_1$-type measurements requires a minimum of 10–15 min and if any signal averaging is done, the time difference is further amplified. The capability of rapidly measuring the exchange rate enables the rate to be measured as a function of time. This opens the door to a wide range of applications previously inaccessible owing to the time resolution of former techniques. A few examples of such applications would be measuring the time rate of change of the water exchange rate after addition of drugs that affect the rate (e.g., parachloromercuribenzene sulfonic acid [10]); monitoring the exchange rate as the temperature is lowered in the freezing of cells; and measuring the exchange rate as sickle cells change from their normal to sickled shape. The present technique also provides simultaneous measurement of cell volume that further extends the domain of useful applications.

A second advantage over the $T_1$-type technique is that the NMR signals from hemoglobin and membrane protons are insignificant in the $T_2$ experiment after about 1.0 ms, as a result of the slow motion of these protons. All of the $T_2$-type data are collected after this time. In the $T_1$ experiment, however, the signal decays with a time constant of about 100 ms (9), which means it significantly contributes to the magnetization that must be measured for the exchange rate calculation. Our estimates agree with those of Fabry and Eisenstadt (11) that at normal hematocrits these protons compose about 8–10% of the total blood signal. In the $T_1$-type experiment this signal must be subtracted out, a correction not required in the $T_2$-type experiment.

This paper presents the theory and application of a $T_2$-type technique employing low $MnCl_2$ concentrations with a detailed error analysis covering the major sources of systematic error. The water exchange rate for normal erythrocytes is determined as well as the activation energy for the exchange process. We discuss the implications of the values obtained and compare them with previous determinations.

## METHODS

### *Blood Sample Preparation*

Fresh blood samples were obtained from healthy donors by venipuncture into Vacutainers anticoagulated with a 1% heparin solution by volume. The concentration of the heparin solution was 1,000 USP U heparin/ml. All samples were used within 6 h of collection. $MnCl_2$ was added directly to the fresh blood from various concentrated stock solutions in quantities $\leq 20$ $\mu$l/ml of blood. The plasma concentration of Mn was 1.7 $\pm$ 0.2 mM in all samples except those prepared to check the effect of high Mn concentration on the measured exchange rate. All the 1.7-mM samples were maintained at approximately 300 mosmol plasma concentration by using a 100-mM $MnCl_2$ stock solution. The stock solutions were always prepared at least 1 wk in advance to reduce the rate at which Mn enters the erythrocyte (11, 12). A significant portion of the Mn binds to serum albumin so that the 1.7 mM total plasma concentration actually corresponds to about 0.8 mM free Mn (13). At this low Mn concentration the measured exchange rate was constant over 5 h, in agreement with the observations of Fabry and Eisenstadt (11). All exchange measurements were made within 30 min of $MnCl_2$ addition, except for studies of the temperature dependence of the exchange rate, completed within 3 h.

Cell volume determinations were made by standard microhematocrit techniques. For each measurement at least two samples of whole blood were centrifuged at 10,000 *g* for 7 min. Duplicate determinations never differed by >0.5%. The resulting microhematocrit reading was corrected by 1.6% for trapped plasma volume (14). Packed cell samples for NMR measurements were centrifuged for 50 min at 1,000 *g*. Every blood sample fell into the pH range of 7.5 $\pm$ 0.1 at 23°C.

To measure the hemoglobin and membrane proton signals, erythrocytes were equilibrated with isotonic $D_2O$ (Stohler Isotope Chemicals Inc., Waltham, Mass., 99.8%). All manipulations involving the isotonic $D_2O$ were carried out in a glove bag filled with extra-dry nitrogen gas and containing an exposed dish of dry phosphorus pentoxide. The cells were centrifuged at 1,000 *g* for 5 min, the supernate was removed, and four additional volumes of isotonic $D_2O$ were added. The sample was sealed and allowed to equilibrate for 30 min and then the process was repeated four more times. The final sample consisted of packed cells.

### *NMR Measurements*

Pulsed NMR measurements were made on a Spin-Lock CPS-2 pulsed spectrometer (Spin-Lock, Ltd., Port Credit, Ontario, Canada) utilizing a Bruker HFX-90 variable field magnet (Bruker Instruments, Inc., Bellerica, Mass.). A homebuilt accessory to the instrument provided for (*a*) blanking of the pulse signal output, (*b*) a continuously variable delay trigger after the 180° pulse of the Carr-Purcell-Meiboom-Gill (CPMG) sequence, and (*c*) an adjustable DC level. The output of the CPS-2 was fed into a Fabri-Tek 1074 instrument computer (Nicolet Instrument Corp., Madison, Wisc.) where up to 16 scans were signal averaged (waiting at least six $T_1$s between scans). The data were then transferred via an Intel 8080A Microprocessor Interface (Intel Corp., Santa Clara, Calif.) to a DEC system-10 computer (Digital Equipment Corp., Marlboro, Mass.). Details concerning the interface are available elsewhere (15).

Measurements were made at 60 MHz in the standard CPMG pulse sequence (16, 17). The continuously variable delay trigger was adjusted so as to sample only the peaks of the spin echoes with the Fabri-Tek. The pulse spacing was measured with a Hewlett-Packard model 5216 12.5 MHz elec-

tronic counter (Hewlett-Packard Co., Palo Alto, Calif.) to within 0.1%. The typical spacing between 180° pulses was 0.120 ms. A 90° pulse was 2.4 μs and the receiver dead time was <15 μs. Phase-sensitive detection was employed and checked to insure linearity.

$H_1$ homogeneity was checked by the method suggested by Farrar and Becker (8). To insure good $H_1$ homogeneity, less than half the coil was filled with sample, which amounted to approximately 50 μl.

High-resolution measurements were made using the Bruker HFX-90 spectrometer. Special attention was given to insuring the slow passage condition (18), minimizing the amount of filtering, optimizing field homogeneity, and proper phase adjustment.

Temperature measurements were made using a Duo-Wrap 36 gauge Cu-constantan thermocouple (Thermo Electric, Co., Inc., Saddle Brook, N.J.) calibrated with a Keithley 160B digital multimeter (Keithley Instruments, Inc., Cleveland, Ohio) against a Mettler FP-5 temperature controller (Mettler Instrument Corp., Princeton, N.J.). The relative error of the calibration was ±0.1°C, and the absolute error within ±0.2°C. The thermocouple was inserted into a melting point capillary-containing heat-sink compound for good thermal conduction. The capillary was then placed in the sample and the temperature monitored until thermal equilibrium was attained. The sample temperature was controlled to ±0.4°C by a Bruker BST 100/700 temperature controller (Bruker Instruments) employing thermally regulated nitrogen gas.

### *Data Analysis*

The data were analyzed on a DEC system-10 computer with the nonlinear regression program, NLE (19), with the two-site exchange expressions given below (see Eqs. 4 and 11) for the absorption and CPMG data, respectively. The program employs the Hartley (20) and Marquardt (21) search algorithms and allows their implementation separately or together.

Experimental curves of samples from the 10 volunteers were composed of at least 250 points. All other experiments were done with over 550 points. Although such a large number of points is not entirely necessary, it should be noted that a closely defined lineshape is important for the nonlinear analysis to accurately detect small changes in the parameters of interest.

## THEORY OF NMR TWO-SITE EXCHANGE

### *Absorption Spectra*

Historically, several equations describing the effect of chemical exchange on NMR spectra have been derived for particular spin systems (22–25). McConnell (26) has modified the Bloch equations to include two-site uncoupled chemical exchange and arrived at the following expression:

$$M = iK[\tau_a + \tau_b + \tau_a\tau_b(\alpha_a P_b + \alpha_b P_a)]/[(1 + \alpha_a\tau_a)(1 + \alpha_a\tau_b) - 1], \quad (1)$$

where

$$\alpha_a = 1/T_{2b} - i(\omega_a - \omega), \quad (2)$$

$$\alpha_b = 1/T_{2b} - i(\omega_b - \omega), \quad (3)$$

in which $M$ contains both the real and imaginary portions of the magnetization. $P_a$ and $P_b$ are the fractions of the total signal in site A and site B, respectively. Likewise, $\omega_a$ and $\omega_b$ are the chemical shifts of the two sites, and $\tau_a$ and $\tau_b$ are the mean lifetimes of the species of interest in each site. $\omega$ is the frequency in radians, and $T_{2a}$ and $T_{2b}$ are the respective transverse relaxation times of the two sites. $K$ is a scaling factor proportional to the product of the gyromagnetic ratio, the $H_1$ field, and the equilibrium magnetization ($M_0$).

Several simplified extensions of Eq. 1 have been derived for limiting cases and are avail-

able in standard NMR references. After some algebraic manipulations and regrouping of Eq. 1, we have derived a general expression for the absorption spectrum in two-site uncoupled exchange:

$$V(\omega) = K(AD + BC)/(C^2 + D^2), \tag{4}$$

where

$$A = \tau_a\tau_b(P_b\omega_a + P_a\omega_b - \omega), \tag{5}$$

$$B = \tau_a + \tau_b + \tau_a\tau_b(P_b/T_{2a} + P_a/T_{2b}), \tag{6}$$

$$C = \tau_b/T_{2b} + \tau_a/T_{2a} + \tau_a\tau_b/T_{2a}T_{2b} - \tau_a\tau_b(\omega_a - \omega)(\omega_b - \omega), \tag{7}$$

$$D = \tau_b(T_{2a} + \tau_a)(\omega_b - \omega)/T_{2a} + \tau_a(T_{2b} + \tau_b)(\omega_a - \omega)/T_{2b}. \tag{8}$$

From considerations of detailed balancing:

$$P_a = 1 - P_b, \tag{9}$$

$$P_a/\tau_a = P_b/\tau_b. \tag{10}$$

*CPMG Spectra*

Woessner (27) has derived the following normalized expression for the effect of two-site exchange on the CPMG decay, assuming no significant chemical shift difference between site A and B.

$$M(t) = [P_{a'}\exp(-t/T_{2a'}) + P_{b'}\exp(-t/T_{2b'})], \tag{11}$$

where

$$1/T_{2a'} = C_1 - C_2, \tag{12}$$

$$1/T_{2b'} = C_1 + C_2, \tag{13}$$

$$P_{b'} = \tfrac{1}{2} - \tfrac{1}{4}[(P_b - P_a)(1/T_{2a} - 1/T_{2b}) + 1/\tau_a + 1/\tau_b]/C_2, \tag{14}$$

$$P_{a'} = 1 - P_{b'}, \tag{15}$$

$$C_1 = \tfrac{1}{2}[1/T_{2a} + 1/T_{2b} + 1/\tau_a + 1/\tau_b], \tag{16}$$

$$C_2 = \tfrac{1}{2}[(1/T_{2b} - 1/T_{2a} + 1/\tau_b - 1/\tau_a)^2 + 4/\tau_a\tau_b]^{1/2}. \tag{17}$$

The parameters have the same meaning as in Eq. 1, and Eqs. 9 and 10 are also applicable. For the nonlinear regression fit, it is also important to add the base line as a variable parameter.

In this study water exchange is characterized by measuring $\tau_a$, the mean lifetime of water in the cell. $\tau_a$ can be related to the water diffusion permeability coefficient $P_d$ (28) by:

$$P_d = V_w/A\,\tau_a, \tag{18}$$

where $V_w$ is the volume of intracellular water, and $A$ is the surface area of the erythrocyte. Water exchange can also be characterized in rate constant notation. For example, the first-order rate constant $k_a$ for water leaving the cell is equal to $1/\tau_a$.

## CALCULATIONS

### *High Resolution Spectra*

Our original approach to the water exchange measurements was based on total line shape (TLS) analysis of blood doped with $MnCl_2$. This method proved to be more time-consuming and less reliable than the CPMG-type analysis. However, the TLS analysis is important because it provides an estimate of the chemical shift induced by the Mn.

In principle, the absorption spectrum of Mn-doped blood can be fit by Eq. 4 using nonlinear regression to obtain $P_a$, $\tau_a$, $T_{2a}$, $T_{2b}$, $\omega_a$, $\omega_b$, a scaling factor, a base line, and a phase adjustment. Even though this may seem a large number of parameters to be able to correctly determine, it turns out that the mathematics of Eq. 4 and the quality of the data require that only $T_{2a}$ be independently determined. But, measuring $T_{2a}$ was the first problem with the TLS analysis. By analyzing the line width of undoped blood and using the rapid exchange approximation of Eq. 4, an estimate of $T_{2a}$ could be made only to within approximately $\pm 15\%$.

A second difficulty with the high resolution approach was that hemoglobin and membrane protons constitute about 8–10% of the observed signal. Although the expected perturbation of the line shape should be slight, it is very difficult to quantify.

The most troublesome difficulty of the high resolution approach was the settling of cells as a result of sample spinning. Even after fibrin was removed from the blood and the spin rate was reduced, cell settling proceeded rapidly. If a sample was shaken to remix the cells, the rate of settling was even more rapid. This made measurements lasting >5–10 min difficult and was the main reason the CPMG method was chosen.

From spectra taken before significant settling had occurred, it was found that the chemical shift difference ($\omega_a - \omega_b$) was insensitive to a broad range of $T_{2a}$ values. A clear upper limit of 3.0 Hz could be set on the induced chemical shift of 1.7 mM $MnCl_2$. It was also satisfying that under the same conditions of temperature and Mn concentration, $\tau_a$ from the TLS analysis was within 5% of the value calculated from the CPMG line fit.

### *CPMG Decay*

The difficulties of the high resolution method are largely overcome by the CPMG experiment. Because the CPMG technique separates the inhomogeneity contribution, it simplifies the direct measurement of $T_{2a}$ (see Results). Also from isotonic $D_2O$ equilibration work, the hemoglobin and membrane proton signals were found to decay too fast to contribute significantly during the time of data acquisition. Calculations with Eq. 11 showed that completely ignoring the hemoglobin and membrane proton signals changed the best-fit $P_a$ and $\tau_a < 0.3\%$. Most importantly, the erythrocyte settling rate is much slower in a nonspinning sample.

By examining Eq. 11 and noting that $P_b = 1 - P_a$, it can be seen that other than a scaling factor and a baseline, only three parameters are required to fit any two-site exchange. The unknown parameters available are $P_a$, $\tau_a$, $T_{2a}$, and $T_{2b}$ ($\tau_b$ and $P_b$ being obtained from Eqs. 9 and 10). It is therefore necessary to measure one of these four parameters independently and for reasons discussed in the Results, $T_{2a}$ was chosen.

To determine the sensitivity of the $T_2$-type technique to changes in $\tau_a$, simulation data were calculated from Eq. 11. The results for a range of $\tau_a$ values are illustrated in Fig. 1.

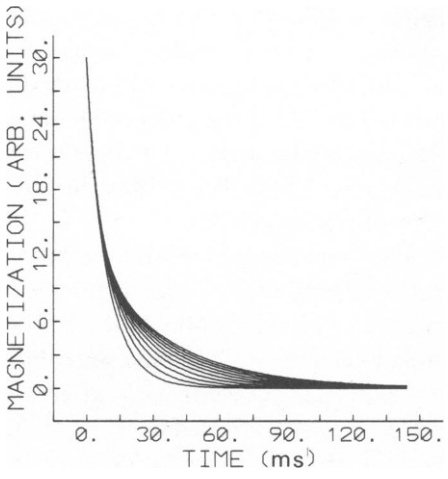


FIGURE 1

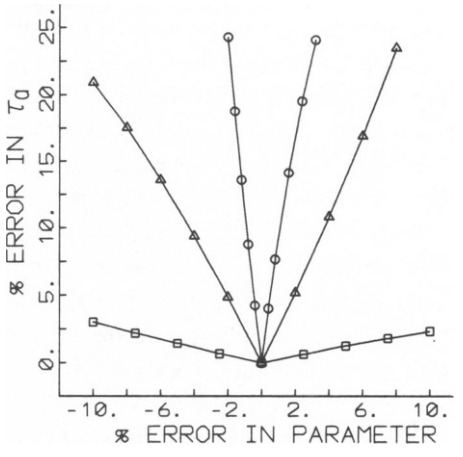


FIGURE 2

FIGURE 1 Simulated two-site exchange CPMG decay for blood doped with $MnCl_2$. Parameter values were $P_a = 0.34$, $\tau_a = 5$ to 50 ms, $T_{2a} = 100$ ms, and $T_{2b} = 5$ ms.
FIGURE 2 Propagation of error in the calculation of $\tau_a$. Parameters are denoted: $T_{2a}$ as squares, $P_a$ as triangles, and $T_{2b}$ as circles.

Analogous graphs were calculated for $P_a$ and $T_{2b}$ to confirm that the CPMG decay would be sensitive to changes in these parameters. Data graphed in this figure indicate that certain portions of the curve are relatively insensitive to changes in $\tau_a$. In obtaining data it is thus important to include a good sampling of points from the sensitive portion. Several authors (28–30) have made independent determinations of $P_a$, $T_{2a}$, $T_{2b}$, the scaling factor, and/or the base line and have used Eq. 12 or a simplified version thereof to obtain $\tau_a$. In these types of calculations, data sampling in the upper portion of the curve would be useless in determining $\tau_a$ and adequate sampling of the sensitive region would be of primary importance.

## RESULTS

### *$T_{2a}$ Measurement*

Other than the scaling factor and base-line parameters, Eq. 11 dictates that only three pieces of information are available from the CPMG exchange curve. Because four parameters are present in the equation, one must be independently measured. Simulation numerical analyses were done to determine how sensitive the $\tau_a$ calculation was to errors in measuring each of the parameters. The results are summarized in Fig. 2. Estimating that $P_a$ could be determined from microhematocrit measurements to about ± 3%, and that $T_{2a}$ and $T_{2b}$ could be measured to about ± 5%, Fig. 2 shows that independently measuring $T_{2a}$ would clearly be the best choice. This can also be seen by examining the relationship of $T_{2a}$ and $T_{2b}$ in Eqs. 14, 16, and 17. In these expressions $1/T_{2a}$ and $1/T_{2b}$ occur together and are either added or subtracted. Because $1/T_{2a}$ is about $10\,s^{-1}$ and $1/T_{2b}$ is about $200\,s^{-1}$, it is not surprising that an error in $T_{2a}$ would not exert much effect.

The most straightforward technique of measuring $T_{2a}$ is to spin down whole blood and measure a packed cell sample. However, a $T_{2a}$ measurement on such a sample would include a contribution from the trapped plasma volume. The effect of the trapped plasma on the observed signal depends on (*a*) the amount trapped, (*b*) the $T_2$ of the trapped plasma, and (*c*) how fast the plasma water exchanges with the intracellular water. Of these three unknowns, only the amount of trapped volume can be readily determined and that in turn depends on the centrifugal force and length of time of centrifugation (14, 31).

Because estimation of the $T_2$ of the trapped volume and its exchange rate with the intracellular water was not possible, an alternate route of measurement was taken to confirm the packed cell determinations. This alternate method consisted of taking CPMG data over the desired temperature range on undoped blood with normal hematocrit. The data were then fit to Eq. 11 using independent measurements of $P_a$, $\tau_a$, and $T_{2b}$. The error induced in $T_{2a}$ from errors in measuring $P_a$, $\tau_a$, and $T_{2b}$ is shown in Fig. 3. $P_a$ was estimated to ± 3% from packed cell volume measurements by standard microhematocrit techniques with correction made for trapped plasma volume. The estimate of $\tau_a$ at a given temperature was from calculations made with NLE by assuming that the $T_{2a}$ from packed cell samples was reasonably accurate (which turned out to be the case). From Fig. 3 it can be seen that $T_{2a}$ is extremely insensitive to the correct value of $\tau_a$, so this first-order estimate was quite adequate. The measurement of $T_{2b}$ over the temperature range studied was made on undoped plasma containing an appropriate concentration of lysed erythrocyte membrane to simulate whole blood conditions. Estimated error of the $T_{2b}$ determination is within ± 5%.

The results of $T_{2a}$ determinations as a function of temperature in packed cell samples are shown in Fig. 4. Each point is the average of three blood samples with two measurements made per sample. The alternate method gave values consistently within 5% of the packed cell method which is within the estimated experimental error. It is interesting to note from Fig. 4 that a full 5% error in $T_{2a}$ would induce but a 1.5% error in $\tau_a$.

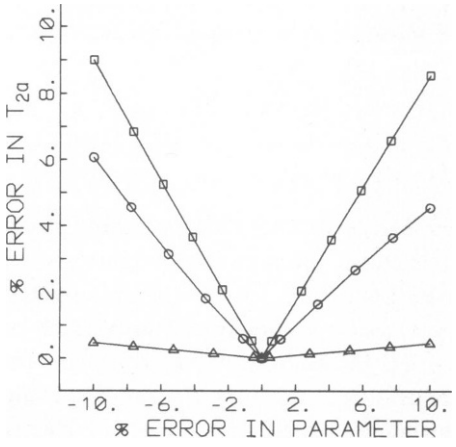


FIGURE 3

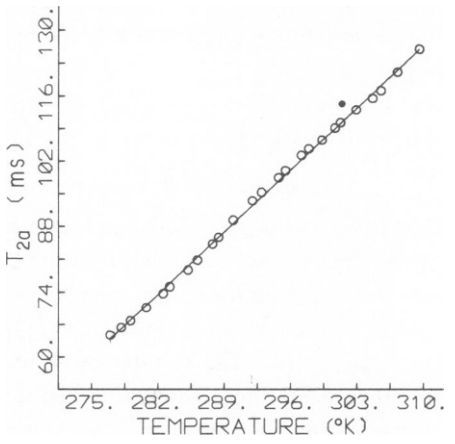


FIGURE 4

FIGURE 3 Propagation of error in the calculation of $T_{2a}$. Parameters are denoted: $\tau_a$ as triangles, $P_a$ as circles, and $T_{2b}$ as squares.

FIGURE 4 Temperature dependence of the transverse relaxation time of water within the erythrocyte.

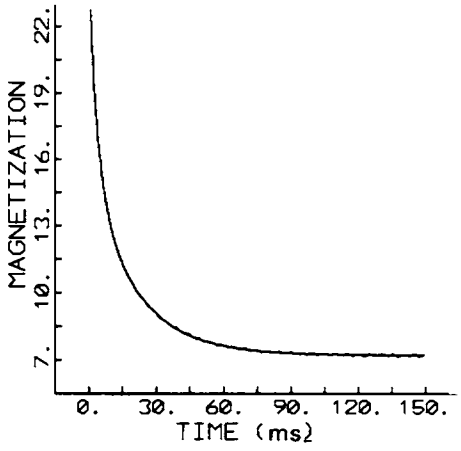


FIGURE 5

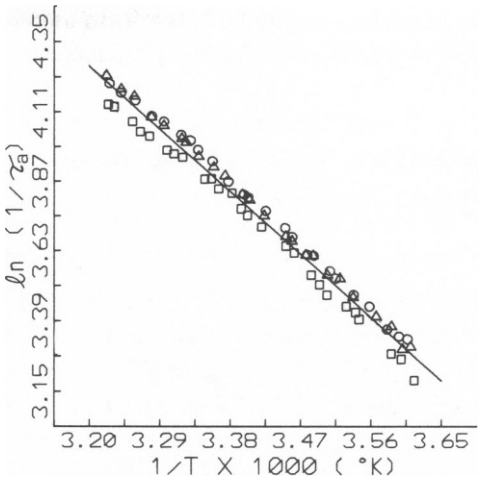


FIGURE 6

FIGURE 5 CPMG decay of blood doped with 1.7 mM $MnCl_2$ with the best fit curve from the nonlinear regression analysis.

FIGURE 6 Arrhenius plot of $\ln(1/\tau_a)$ vs. reciprocal temperature.

### *$\tau_a$ Determination*

Blood samples were collected from 10 donors (5 men and 5 women) with five measurements of $\tau_a$ made on each sample. No special attention was given as to the time of day of sample collection, whether after meals, exercise, or otherwise. Results from a typical CPMG experiment used to calculate $\tau_a$ are shown in Fig. 5. It should be pointed out that the best fit curve from the nonlinear fit has been drawn through the data and is indistinguishable from the experimental plot. The mean value of $\tau_a$ obtained from the samples of the 10 donors at 23°C was 21.0 ± 0.6 (SE).

### *Activation Energy*

An Arrhenius plot of $\ln(1/\tau_a)$ vs. reciprocal temperature is shown in Fig. 6. The data are from the blood of one donor but collected on three different days. Each point is an average of two $\tau_a$ determinations. The variance of the $\tau_a$ values was approximately

TABLE I
ACTIVATION ENERGY RESULTS

| Run | No. of points | $E_a$ |
|---|---|---|
| | | *kcal* |
| 1 | 25 | 4.77 |
| 2 | 25 | 4.84 |
| 3 | 25 | 4.76 |

Average of three determinations—4.79 ± 0.03 (SE).
Value from least squares fit of combined data—4.77 ± 0.07 (SE).

constant over the temperature range studied so a nonweighted least squares analysis was used to find $E_a$ (32). Results are summarized in Table I.

*Cell Volume*

Simultaneous estimates of cell volume can be made from the nonlinear regression values of $P_a$ according to Eq. 19.

$$\text{Hematocrit} = P_a/(V_i + (1 - V_i)(V_p)(P_a)) \quad (19)$$

where $V_i$ is the fraction of intracellular volume that is water and $V_p$ is the fraction of plasma volume that is water. Results of hematocrits calculated from Eq. 19 with $V_i = 0.71$ (33) and $V_p = 0.95$ (34) agreed within 3% with independent microhematocrit measurements corrected for trapped plasma volume.

## ERROR ANALYSIS

Although random error can be estimated from multiple measurements, several sources of potential systematic error must be considered. How such errors are dealt with in measuring $T_{2a}$ has already been discussed. This section deals with potential systematic errors in measuring $\tau_a$ and $E_a$.

Possible sources of error in measuring $\tau_a$ can arise from (*a*) incorrect steady-state base-line determination, (*b*) errors in the independent measurements of $P_a$, $T_{2a}$, and/or $T_{2b}$, (*c*) nonexponential contributions to $T_{2a}$ and $T_{2b}$, (*d*) the use of high concentrations of $MnCl_2$, and (*e*) a $MnCl_2$-induced chemical shift. Although these factors can contribute a significant error, correct experimental design and data analysis reduce their cumulative effect to about ± 2%.

The first and very important source of systematic error is improper base-line determination. Vold et al. (35) have shown that even under ideal CPMG conditions, the steady-state base line of the CPMG decay does not conform to the base of the spin echoes. He further points out that ignoring this steady-state value could readily result in systematic errors of 12% in $T_2$. The accurate measurement of $\tau_a$ is even more sensitive to accurate base-line measurement. A base-line error of 2% of $M_0$ can yield as much as a 40% error in $\tau_a$. Although these small base-line errors can lead to serious error in $\tau_a$, sufficient accuracy can be achieved in the base-line measurement in two ways. First, the CPMG decay signal can be monitored until the steady-state base line is sufficiently sampled. Second, the base line can be fit in a nonlinear analysis by the criterion of least squared error. We have employed both techniques, and the base line was calculated within 0.05% at a 95% confidence interval. The resulting error in $\tau_a$ was directly determined from the nonlinear fit and amounted to $< 0.3\%$.

An analogous source of error in using Eq. 11 with $T_1$-type data (11) would arise from error in the determination of the equilibrium magnetization $M_0$. In the customary analysis of $T_1$-type data using semilog plots, the magnetization ($M_z$) is subtracted from $M_0$. This subtraction means that a systematic error in $M_o$ would effectively contribute as a base-line error. We did not do simulation analyses for the propagation of such systematic error because of variety of approximations of Eq. 11 which have been used. Such calcula-

tions would seem warranted in a $T_1$-type analysis in light of the results of the effect of base-line error on the $T_2$-type analysis.

It is also important to point out that as $M_z$ approaches $M_0$, the data in the semilog plot format is calculated from the difference of two relatively large numbers, leading to extensive scattering in this portion of the curve (11). To obtain data within reasonable error limits, data sampling often must be limited to the first 1–1.5 decades of decay. Although the importance of the remaining omitted data points will vary according to the particular values of the exchange parameters, in the present $\tau_a$ determination, these points are useful in the calculation of $P_a$ and $T_{2a}$.

It should be noted that in the nonlinear regression analysis, $T_1$-type data can be analyzed in either the regular or semilog data format. With the nonlinear approach, $M_0$ could be fit by the least squares criterion which, for the same quality of data, would provide a more accurate determination.

A second source of systematic error in $\tau_a$ in the $T_2$-type experiment arises from errors in the independent measurements of $P_a$, $T_{2a}$, and/or $T_{2b}$. The contribution of errors in these parameters to error in $\tau_a$ has already been shown in Fig. 2. Particular attention should be paid to $T_{2b}$, which most likely would not be able to be independently measured much better than ±5%. These data suggest that if abbreviated forms of Eq. 11 are used, care should be taken to determine the propagation of errors in the independently measured parameters. As previously mentioned, the present study only requires the independent measurement of $T_{2a}$.

The third potential source of error arises from the contribution of various relaxation mechanisms to $T_{2a}$ and $T_{2b}$. The accurate determination of $T_2$ has often been plagued by contributions from field inhomogeneity, paramagnetic substances, diffusion, etc. One of the significant attributes of Eq. 11 in describing exchange is that such contributions to $T_{2a}$ and $T_{2b}$ do not have to be separately determined. The only requirement is that an effective transverse relaxation time can be measured.

The likelihood of errors caused by diffusion processes has been examined in some depth. There appears to be only one possible but unlikely case in which bounded diffusion could present a problem. Usually, such contributions can be absorbed into an effective $T_2$ (8). However, it is possible that diffusion in a bounded region could introduce nonexponential character into the CPMG decay. Theoretical calculations of the effect of bounded diffusion on 90°–180° spin echo measurements have been made for planar cylindrical, and spherical geometries (36–39). Particular cases can be evaluated from equations provided in these sources. In the current $\tau_a$ measurements, calculations with Eq. 23 of reference 36 using the thickness of the erythrocyte (about 2.1 μm) and a CPMG pulse spacing of 0.12 ms, indicate that such bounded diffusion could not contribute any significant nonexponential character to the curve.

In addition, two straightforward measurements can be used to check for nonexponentiality. The first is the obvious direct analysis of the CPMG decay to determine if the data fits a single exponential. In this work, exponential decays were observed within experimental error for packed erythrocytes, plasma, and plasma with suspended erythrocyte membranes. Secondly, if $\tau_a$ is being calculated with Eq. 11, $T_1$-type data can also be taken. Inasmuch as $T_1$-type data are not susceptible to such diffusion errors, it should agree with the

$T_2$-type data if bounded diffusion has had no effect. In summary, except in rare instances, determination of $\tau_a$ from Eq. 11 is completely independent of the relaxation mechanisms which contribute to an effective $T_{2a}$ or $T_{2b}$.

The fourth source of potential systematic error in measuring $\tau_a$ is the use of too high a concentration of $MnCl_2$. The effect of $MnCl_2$ concentration on the measured value of $\tau_a$ is shown in Fig. 7. The arrows in the figure indicate the $MnCl_2$ concentrations used in $T_2$-type experiments previous to this work. It can be seen that these high concentrations induce a 35–45% systematic error in the $\tau_a$ measurement. This inhibition of water exchange by Mn, as indicated in the figure, is also supported by the high Mn concentration data of Fabry and Eisenstadt (11).

This study employed a 1.7 mM total $MnCl_2$ concentration, which corresponds to about 0.8 mM free Mn. There are several reasons to believe that $\tau_a$ measured at this low concentration is not significantly influenced by the Mn concentration. First, the data in Fig. 7 appear to be approaching the $\tau_a$ of the 1.7 mM $MnCl_2$ concentration as a limiting value. Using the $T_1$-type technique, Fabry and Eisenstadt have decreased the total $MnCl_2$ concentration to as low as 0.2 mM and shown that the results were consistent with values obtained up to about 5 mM. The possible perturbation of the membrane from 0.2 mM Mn must be considered in light of the fact that the membrane is already exposed to about 2.0 mM concentration of magnesium, which is extremely similar to Mn in terms of its physiological effects on erythrocytes (12). In addition, Fabry has made measurements without Mn using $T_1$-type data of $^{17}O$ which indicate that $\tau_a$ is >20 ms (in good agreement with our results at the same temperature). These facts point to a very small or negligible effect of low concentration of Mn on $\tau_a$.

The final potential source of systematic error in $\tau_a$ is the presence of a Mn-induced chemical shift difference between the intracellular and plasma water. This is a potential source of error because Eq. 11 assumes no chemical shift difference between the two sites. High resolution total line-shape analysis indicates that up to 3 mM total $MnCl_2$ concentra-

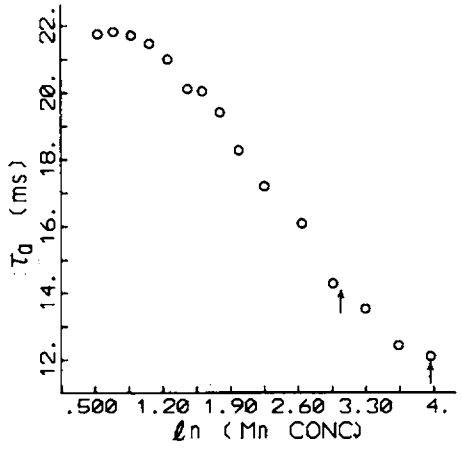


FIGURE 7 The effect of $MnCl_2$ concentration on the measured value of $\tau_a$. The arrows indicate the concentrations used by previous investigators. This work is done at 1.7 mM which corresponds to the left most point on the graph.

tion, the induced chemical shift is certainly <3 Hz. Carver and Richards (40) have derived an expression for the CPMG echo heights which includes a chemical shift difference. Using their Eq. 4, the difference between calculated curves for a 3-Hz and 0-Hz chemical shift difference was found to affect $\tau_a$ < 1%.

Finally, some discussion is warranted on the validity of the two-site exchange model. Eq. 11 assumes that the time for water to diffuse between cell boundaries in the cell or plasma is short compared to the lifetime of the water in that compartment. Pagenelli and Solomon (41) have shown this to be the case inside the cell, and Fabry and Eisenstadt (11) have verified this assumption for the intracellular and plasma compartments. One additional assumption of the two-site model is that a negligible amount of relaxation occurs during the transit of water across the membrane. Because transverse relaxation times are sensitive to low-frequency molecular motions, it is conceivable that some sort of molecular interaction with membrane components might contribute to water relaxation. Two experimental findings indicate that if this occurs its effect is negligible within experimental error. First, the curve calculated from Eq. 11 provides an excellent fit to the experimental data (Fig. 5). Second, the $T_2$-type data are in excellent agreement with $T_1$-type results (11), not susceptible to low frequency relaxation mechanisms.

The precision of the $\tau_a$ measurements on a given blood sample was within 2%. The precision of the measurements made on 10 samples from different donors was <2.9%. We estimate that the cumulative systematic error contribution of the above-mentioned factors to be <2.5%. Within this framework, the values of $\tau_a$ should have a total error of approximately 3–5%.

*Systematic Error in Activation Energy Determination*

In addition to random errors in the apparent activation energy, which can be calculated from repeated slope determinations on different sets of data, systematic errors in $E_a$ can result from systematic errors in $\tau_a$ or temperature. The following expression has been derived from the Arrhenius equation to describe how systematic error in $\tau_a$ and temperature are propagated into $E_a$:

$$(\sigma_{Ea}/Ea)^2 = (T_2/\Delta T)^2(\sigma_{T_1}/T_1)^2 + (T_1/\Delta T)^2(\sigma_{T_2}/T_2)^2 + (1/\Delta \ln k)^2[(\sigma_{k_1}/k_1)^2 + (\sigma_{k_2}/k_2)^2], \quad (20)$$

where $k_1 = 1/\tau_a$ at a certain temperature ($T_1$), etc. If the error in $k_1$ is approximately equal to the error in $k_2$ and the error in $T_1$ is about the same as in $T_2$, then the equation reduces to an expression derived by Binsch (42). Eq. 20 is applicable to any $E_a$ calculation and brings out an important and generally well-known point concerning experimental design: to minimize the effects of systematic error in $\tau_a$ or temperature on $E_a$, a wide range of both $\tau_a$ and temperature should be sampled. Experimentally, only the temperature range can be chosen. As a result of the practical temperature boundaries of biological measurements, we have sampled from 3° to 37°C.

The major source of systematic error in $E_a$ is from systematic error in $\tau_a$. In this work, we estimate $T$ to be within 0.3°K in absolute accuracy and possible systematic errors in $\tau_a$ to be < ±2.5%. This results in a propagated error in $E_a$ of ±4.5%. If we had

sampled only half the temperature range, the same errors would have yielded an ±8.4% propagated systematic error in $E_a$.

## DISCUSSION

### *Comparison with Previous $\tau_a$ Results*

Previous measurements of $\tau_a$ can be divided into two groups: those that used high Mn concentrations (20–53 mM) and those that used low Mn concentrations or no Mn. The results of the high Mn concentration studies are summarized in Table II. The values from this work at the appropriate temperature were calculated from the activation energy data in Table I. All of the other studies in Table II used simplified versions of Eq. 12, which result from $T_{2a} \gg T_{2b}$, and $T_{2b}/\tau_b$ being <0.3 or $\ll$1.0 (30). The high Mn concentrations were required for these simplifying conditions. Without considering other possible differences, the disagreement between these studies and the present one can be reconciled on the basis of the systematic error induced from the high Mn concentration (Fig. 7).

The results of studies employing low concentrations of Mn or no Mn are shown in Table III. There is excellent agreement between this work and the proton and $^{17}O$ results of Fabry and Eisenstadt. The $^{17}O$ $T_1$ of Shporer and Civan (9), though somewhat lower, is in reasonable agreement with that of Fabry and Eisenstadt (11). Because the $^{17}O$ $T_1$s of both the plasma and intracellular water fractions are shorter than $\tau_a$, the $^{17}O$ technique becomes insensitive to $\tau_a$ around 23°C (9, 11).

Andrasko (43) has measured $\tau_a$ using pulsed gradient NMR. He employs several simplifications of the general expression for the dependence of $\tau_a$ on measured diffusion coefficients to arrive at his Eq. 4, from which $\tau_a$ is calculated. His value of 17 ms at 24°C is also in reasonable agreement with this work. However, it must be pointed out that Andrasko's equation requires the independent measurement of the diffusion coefficient of plasma water. A conservative estimate of the error in such a measurement would be ±5%. Such an error would produce a ±20% systematic error in $\tau_a$ calculated from Andrasko's equation. The usefulness of the pulsed gradient technique is thus dependent on the very accurate determination of the plasma water diffusion coefficient.

The last $\tau_a$ values in the table are from isotopic tracer measurements. This technique involves an elaborate flow tube apparatus and a demanding experimental procedure (6). The precision of the most recent rigorous estimate of $\tau_a$ by this technique is ±24% SD (6). Sources of systematic error in the $T_2$-type technique have already been discussed. Sources of systematic error in the tracer experiment have been discussed by Solomon (4) and at

TABLE II

$\tau_a$ MEASUREMENTS USING HIGH Mn CONCENTRATIONS

| Method | Temperature | Mn concentration | $\tau_a$ | $\tau_a$ (this work) | Reference |
|---|---|---|---|---|---|
| | *°C* | *mM* | *ms* | *ms* | |
| $T_2(^1H)$ | 37 | 25 | 8.2 ± 0.11 | 14.8 | 62 |
| $T_2(^1H)$ | 37 | 20 | 6.0 ± 0.5 | 14.8 | 63 |
| $T_2(^1H)$ | 25 | 35, 53 | 11.0 ± 0.5 | 20.2 | 61 |
| $T_1(^1H)$ | 25 | 20 | 17.7 ± 0.3 | 20.2 | 61 |

TABLE III

$\tau_a$ MEASUREMENTS WITH LITTLE OR NO Mn

| Method | Temperature | Mn conc | $\tau_a$ | $\tau_a$ (this work) | Reference |
|---|---|---|---|---|---|
| | °C | *mM* | *ms* | *ms* | |
| $T_1(^1H)$ | 25 | as low as <0.5 | 21.7 ± 2.5 | 20.2 | 36 |
| $T_1(^{17}O)$ | 25 | 0 | >20.0 | 20.2 | 36 |
| $T_1(^{17}O)$ | 25, 37 | 0 | 16.7, 9.35 | 20.2, 14.8 | 60 |
| Pulsed gradient | 24 | 0 | 17 | 20.9 | 37 |
| Isotope tracer | 22 | 0 | 11.0 ± 2.7 | 21.9 | 59 |

least two significant sources deserve attention. First is the presence of unstirred layers (7). Measurements of the thickness of such layers around erythrocytes have been made and their effect on the measured water permeability established (41). It is, however, difficult to estimate the exact systematic error induced from the unstirred layers or to check their accurate measurement. A second source of systematic error is in approximating water diffusion with tritiated water. Wang (44) has found that $HH^{18}O$ has a diffusion coefficient 14% larger than that of tritiated water. Tracer measurements of $\tau_a$ have incorporated a correction for this error based on Wang's results, but other authors are not entirely in agreement concerning either the magnitude or the effects of this difference (45–47). Clearly, the accurate calculation of $\tau_a$ by tracer methods is dependent on the accurate measurement of the diffusion coefficient of both water and tritiated water. As an examination of Table IV shows, the present results for $\tau_a$ are in much better agreement overall with the other NMR results. The above-mentioned sources of systematic error in the tracer technique could conceivably contribute to this difference.

*Comparison of Activation Energy Results*

Previously reported values of the activation energy for water exchange and the results of this work are summarized in Table III. The reported errors in $E_a$ are SDs or SEs derived from least squares analyses of Arrhenius plots and do not contain estimates of systematic error. For comparison, the result of this study is listed with the SE from the three measurements of $E_a$. The proton $T_2$ study of Morariu (30) is complicated by a systematic

TABLE IV

COMPARISON WITH ACTIVATION ENERGY MEASUREMENTS OF OTHERS

| Method | Temperature range | No. of points per measurement | No. of measurements | $E_a$* | Reference |
|---|---|---|---|---|---|
| | °C | | | *kcal* | |
| $T_2(^1H)$ | 8 | 5 | ? | 6.0 − 8.0 | 63 |
| $T_1(^{17}O)$ | 14 | 13 | 1 | 8.7 ± 1.0 | 60 |
| Tracer | 34 | 23 | 1‡ | 6.0 ± 0.2 | 94 |
| This work | 34 | 25 | 3 | 4.79 ± 0.03 | — |

*Error estimates are SD or SE from the least squares fit and do not include estimates of systematic error.
‡Assuming all the data in Fig. 4 of reference 2 were fit together.

error of unknown amount from the high Mn concentration employed. In addition, only a narrow temperature range is sampled. As previously mentioned, the $^{17}O$ study is only sensitive to $\tau_a$ over a restricted temperature range.

The isotopic tracer measurements were made over an adequate temperature range but showed considerable scatter. The data in Fig. 4 of Viera et al. (48) were apparently all analyzed in a single least squares fit. On account of limitations in availability of sufficient quantities of blood, data were taken at only three temperatures. Comparison between our NMR and the tracer results are made difficult by the lack of any estimate of systematic errors in the tracer technique. For instance, a systematic error of only 10% in measuring $\tau_a$ by the tracer method would yield an error of over 17% in $E_a$ (see Error Analysis) which alone would account for the difference between the two $E_a$ values.

One of the primary goals of this study was the accurate determination of $E_a$. The $T_2$-type technique requires <0.5 ml of blood for a complete experiment in which about 25 $\tau_a$s are measured in <3 h, most of that time being required for temperature equilibration. It is of particular interest that this $E_a$ value is extremely close to the 4.8 kcal activation energy of bulk water diffusion (45). This would imply that by whatever means the water traverses the membrane the barrier it experiences is virtually the same magnitude as in diffusional flow of pure water. The activation energy for water diffusion through a lipid bilayer has been determined to be 12–14 kcal (49, 50). Thus, this $E_a$ of 4.79 kcal would be inconsistent with significant water flow through the lipid portion of the membrane.

### *Advantages and Applications of the* $T_2$*-Type Technique*

The advantages of the $T_2$-type technique as described here are as follows: (*a*) speed—on a given sample $\tau_a$ can be measured every 3 s; (*b*) small sample volume—this work used 50-$\mu$l samples; (*c*) technical simplicity—an aliquot of $MnCl_2$ stock solution is added to whole blood, and measurements are done with the standard CPMG pulse sequence; (*d*) precision—within 2% (SE) for repeated measurements; (*e*) simultaneous measurement of the cell volume; (*f*) ease of signal averaging; and (*g*) lack of complications from unstirred layers or signals from hemoglobin and membrane protons.

These advantages enable $\tau_a$ measurements to be extended to several new applications. The ability to monitor cell volume changes means that this technique would be a suitable alternative to light scattering in following such changes in solute permeability studies (29). The simultaneous measurement of $\tau_a$ and $P_a$ enables the product $P_dA$ to be directly measured over desired experimental conditions (27). As long as $\tau_a$ is intermediate between $T_{2a}$ and $T_{2b}$, it will be sensitive to calculation by Eq. 11. The $T_2$-type technique can therefore be applied to a variety of situations in which this condition is satisfied or can be satisfied by paramagnetic doping, deoxygenation, and/or other techniques which alter the transverse relaxation time.

The speed and simplicity of this technique allows its routine application to the measurement of $\tau_a$ as a function of time. This application is important for a variety of experimental studies, including precisely measuring activation energies in a relatively short time. Studies in this lab are underway monitoring $\tau_a$ with time as the erythrocyte is exposed to drugs that can alter the water exchange rate (10, 51).

This work was supported by grants from the National Institutes of Health and the Schering Foundation. J. L. P. wishes to thank the Insurance Medical Scientist Scholarship Fund for their financial assistance.

## REFERENCES


1. FORSTER, R. F. 1971. The transport of water in erythrocytes. *Curr. Top. Membranes Trans.* **2**:41.
2. SHA'AFI, R. I., and C. M. GARY-BOBO. 1973. Water and nonelectrolyte permeability in Mammalian Red Cell Membranes. *Prog. Biophys. Mol. Biol.* **26**:103.
3. STEIN, W. D. 1967. The Movement of Molecules Across Cell Membranes. Academic Press Inc., New York.
4. SOLOMON, A. K. 1968. Characterization of biological membranes by equivalent pores. *J. Gen. Physiol.* **51**: 335s.
5. RICH, G. T., R. I. SHA'AFI, A. ROMUALDEZ, and A. K. SOLOMON. 1968. Effect of osmolality on the hydraulic permeability coefficient of red cells. *J. Gen. Physiol.* **52**:941.
6. BARTON, T. C., and D. A. J. BROWN. 1964. Water permeability of the fetal erythrocyte. *J. Gen. Physiol.* **47**: 839.
7. DAINTY, J. 1963. Water relations of plant cells. *Adv. Bot. Res.* **1**:279.
8. FARRAR, T. C., and E. D. BECKER. 1971. Pulse and Fourier Transform NMR. Academic Press Inc., New York. 20–29 and 43–44.
9. SHPORER, M., and M. M. CIVAN. 1975. NMR study of $^{17}O$ from $H_2{}^{17}O$ in human erythrocytes. *Biochim. Biophys. Acta.* **385**:81.
10. MACEY, R. I., and R. E. L. FARMER. 1970. Inhibition of water and solute permeability in human red cells. *Biochim. Biophys. Acta.* **211**:104.
11. FABRY, M. E., and M. EISENSTADT. 1975. Water exchange between red cells and plasma. *Biophys. J.* **15**:1101.
12. WEED, R. I., and A. ROTHSTEIN. 1961. The uptake of divalent manganese ion by mature normal red blood cells. *J. Gen. Physiol.* **44**:301.
13. MILDVAN, A. S., and M. COHN. 1963. Magnetic resonance studies of the interaction of the manganous ion with bovine serum albumin. *Biochemistry.* **2**:910.
14. GIBERMAN, E. 1973. Determination of the trapped volume in a pellet of red blood cells. *Experientia (Basel).* **29**:1083.
15. ABRAMSON, M. J., and J. H. GOLDSTEIN. Design and implementation of an economical instrument-computer interface based on the SDK-80 microcomputer. *Comput. & Chem. Biochem. Res.* In press.
16. CARR, H. Y., and E. M. PURCELL. 1954. Effects of diffusion on free precession in nuclear magnetic resonance experiments. *Phys. Rev.* **94**:630.
17. MEIBOOM, S., and D. GILL. 1958. Proton relaxation in water. *Rev. Sci. Instrum.* **29**:688.
18. EMSLEY, J. W., J. FEENEY, and L. H. SUTCLIFFE. 1966. High Resolution Nuclear Magnetic Resonance Spectroscopy. Pergamon Press Ltd., Oxford.
19. BLUMENSTEIN, B. 1975. Personal Communication.
20. HARTLEY, H. O. 1961. The modified Gauss-Newton method for the fitting of non-linear regression functions by least squares. *Technometrics.* **3**:269.
21. MARQUARDT, D. W. 1963. An algorithm for least-squares estimation of non-linear parameters. *J. Soc. Ind. Appl. Math.* **11**:431.
22. GUTOWSKY, H. S., and C. H. HOLM. 1956. Rate processes and nuclear magnetic resonance spectra. II. Hindered internal rotation of amides. *J. Chem. Phys.* **25**:1228.
23. GRUNWALD, E., A. LOWENSTEIN, and S. MEIBOOM. 1957. Rates and mechanisms of protolysis of methylammonium ion in aqueous solution studied by proton magnetic resonance. *J. Chem. Phys.* **27**:630.
24. ALLERHAND, A., and H. S. GUTOWSKY. 1964. Spin echo studies of chemical exchange. I. Some general aspects. *J. Chem. Phys.* **41**:2115.
25. ALLERHAND, A., H. S. GUTOWSKY, J. JONAS, and R. A. MEINZER. 1966. New methods for determining chemical exchange rates. *J. Am. Chem. Soc.* **88**:3185.
26. MCCONNELL, H. M. 1958. Reaction rates by nuclear magnetic resonance. *J. Chem. Phys.* **28**:430.
27. HAZELWOOD, C. F., D. C. CHANG, B. L. NICHOLS, and D. E. WOESSNER. 1974. Nuclear magnetic resonance transverse relaxation times of water protons in skeletal muscle. *Biophys. J.* **14**:583.
28. CHIEN, D. Y., and R. I. MACEY. 1977. Diffusional water permeability of red cells independence on osmolality. *Biochim. Biophys. Acta.* **464**:45.
29. CONLON, T., and R. OUTHRED. 1972. Water diffusion permeability of erythrocytes using a nuclear magnetic resonance technique. *Biochim. Biophys. Acta.* **288**:354.
30. MORARIU, V. V., and G. BENGA. 1977. Evaluation of a nuclear magnetic resonance technique for the study of water exchange through erythrocyte membranes in normal and pathological subjects. *Biochim. Biophys. Acta.* **469**:301.
31. ZIPP, A., T. L. JAMES, I. D. KUNTZ, and S. B. SHOHET. 1976. Water proton magnetic resonance studies of normal and sickle erythrocytes—temperature and volume dependence. *Biochim. Biophys. Acta.* **428**:291.

32. DRAPER, N., and H. SMITH. 1966. Applied regression analysis. John Wiley & Sons, Inc., New York. 264–273.
33. KESSLER, E., M. R. LEVY, and R. L. ALLEN. 1961. Red cell electrolytes in patients with edema. *J. Lab. Clin. Med.* **57**:32.
34. DAVIS, F. E., K. KENYON, and J. KIRK. 1953. A rapid titrimetric method for determining the water content of human blood. *Science (Wash. D.C.).* **118**:276.
35. VOLD, R. L., R. R. VOLD, and H. E. SIMON. 1973. Errors in measurements of transverse relaxation rates. *J. Magn. Res.* **11**:283.
36. KLANDER, J. R., and P. W. ANDERSON. 1962. Spectral diffusion decay in spin resonance experiments. *Phys. Rev.* **125**:912.
37. TANNER, J. E., and E. O. STEJSKAL. 1968. Restricted self-diffusion of protons in colloidal systems by the pulsed-gradient, spin-echo method. *J. Chem. Phys.* **49**:1768.
38. ROBERTSON, B. 1966. Spin echo deday of spins diffusing in a bounded region. *Phys. Rev.* **151**:273.
39. NEWMAN, C. H. 1974. Spin echo of spins diffusing in a bounded medium. *J. Chem. Phys.* **60**:4508.
40. CARVER, J. P., and R. E. RICHARDS. 1972. A general two-site solution for the chemical exchange produced dependence of $T_2$ upon the Carr-Purcell pulse separation. *J. Magn. Res.* **6**:89.
41. PAGENELLI, C. V., and A. K. SOLOMON. 1957. The rate of exchange of tritiated water across the human red cell membrane. *J. Gen. Physiol.* **41**:259.
42. BINSCH, G. 1975. Dynamic Nuclear Magnetic Resonance Spectroscopy. Academic Press Inc., New York. 45.
43. ANDRASKO, J. 1976. Water in agarose gels studied by nuclear magnetic resonance relaxation in the rotating frame. *Biochim. Biophys. Acta.* **428**:304.
44. WANG, J. H. 1965. Self diffusion coefficients of water. *J. Phys. Chem.* **69**:4412.
45. GRAUPNER, K., and E. R. S. WINTER. 1952. Self-diffusion coefficients of liquids. *J. Chem. Soc.* 1145.
46. KOHN, P. G. 1965. Tables of some physical and chemical properties of water. *Symp. Soc. Exp. Biol.* **19**:3.
47. KING, V. 1969. A study of the mechanism of water transfer across frog skin by a comparison of the peremability of the skin to deuterated and tritiated water. *J. Physiol. (Lond.).* **200**:529.
48. VIERA, F. L., R. I. SHA'AFI, and A. K. SOLOMON. 1970. The state of water in human and dog red blood cell membranes. *J. Gen. Physiol.* **55**:451.
49. REDWOOD, W. R., and D. A. HAYDON. 1969. Influence of temperature and membrane composition on the water permeability of lipid bilayers. *J. Theoret. Biol.* **22**:1.
50. PRICE, H. D., and T. E. THOMPSON. 1969. Properties of lipid bilayer membranes separating two aqueous phases: temperature dependence on water permeability. *J. Mol. Biol.* **41**:443.
51. NACCACHE, P., and R. I. SHA'AFI. 1974. Effects of PCMBS on water transport across biological membranes. *J. Cell. Physiol.* **83**:449.